

# BURIED SPHERICAL SHELLS LOCALIZATION IN PRESENCE OF PHASE UNCERTAINTIES

Zineb SAIDI<sup>(1)</sup>, Salah BOURENNANE<sup>(2)</sup>

<sup>(1)</sup>ESSTIN / UHP - Nancy 1, 2, rue Jean Lamour, 54 519 VANDOEUVRE les Nancy cedex  
phone: + (33) 3 83 68 51 39, email: zmeheisa@uhp-nancy.fr

<sup>(2)</sup>Institut Fresnel, UMR CNRS 6133-EGIM, D.U. de saint Jérôme, 13 397 Marseille Cedex 20, France  
phone: + (33) 4 91 28 80 38, email: salah.bourennane@egim-mrs.fr

## ABSTRACT

*Buried object localization in presence of sensor phase errors is presented in this study. Phase errors are introduced by the moving of the sensor array from their original positions during the experiment which gives an erroneous object localization. To solve the problem, an objective function is defined using the exact solution of the scattered acoustic field in the MUSIC method. The DIRECT algorithm (DIviding RECTangles) is used to seek the minimum of this function. The method provides estimation of the bearings and ranges of all buried objects as well as the phase error of each sensor in the observing array. Performances of the proposed method are investigated on experimental data recorded during underwater acoustic experiments.*

## 1. INTRODUCTION

Most array processing techniques are based on the assumption that the shape of the array remains unchanged (the well known sensor positions)[6], [7], [8]. This assumption permits the use of simplified array signal processing techniques. The MUSIC method [10] is a subspace array signal processing technique where the main assumption is a linear sensor array and it is used to estimate the bearing sources. However in practice, the shape of a sensor array, such as flexible towed array and bottom mounted array, is deformed due to the fluctuations in ship maneuvering, underwater currents and swells, and so on. These cause phase errors in the received signals.

Several methods, to estimate the phase errors related to the use of deformed sensor array, were proposed in the literature [1], [2], [5]. The proposed method in [5] uses the sources with known locations as reference sources to correct the positions of the sensors. In [1] the authors assume that the shape of the sensor array is known. Furthermore, those methods consider that the objects are located in the farfield region of sensor array. In such case the range objects are infinite and are not taken into account. This assumption is not valid in the nearfield region of the array.

In this study, we address the problem of a simultaneous estimating of the bearing and the range objects in presence of sensor random phase errors with no prior knowledge of sensor array shape as in [1] and [2] and does not require knowledge of the locations of any source as in [5]. Thus, the idea is to use the spatial complexities of the scattered field to form an acoustic model that we used in the MUSIC method [10]. The received signals are wideband and correlated, thus we apply a frequential smoothing [9] in order to decorrelate them. Then, we define an objective function with multiple

variables which represent the phase errors and the bearing and the range objects. This objective function is based on the orthogonality property between the object subspace and the noise subspace and to minimize this function, we propose to use the DIRECT (DIviding RECTangle) algorithm [4].

The organization of this study is as follows : problem formulation is presented in Section 2. In Section 3, the objective function of multiple variables is defined. In Section 4, the experimental setup is presented. Experimental results supporting our conclusions and demonstrating our method are provided in section 5. Finally, conclusions are presented in Section 6.

Throughout the paper, lowercase boldface letters represent vectors, uppercase boldface letters represent matrices, and lower and uppercase letters represent scalars. The superscript "T" is used for transpose operation and the superscript "+" is used to denote complex conjugate transpose.

## 2. PROBLEM FORMULATION

We consider a flexible array of  $N$  sensors (figure 1) which received the wideband signals scattered from  $P$  objects ( $N > P$ ) in the presence of an additive Gaussian noise and sensor phase errors. The received signals are grouped in the vector  $\mathbf{r}$  given, in the frequency domain, by

$$\mathbf{r}(f_n, \boldsymbol{\theta}, \boldsymbol{\rho}, \boldsymbol{\phi}) = \mathbf{A}_p(f_n, \boldsymbol{\theta}, \boldsymbol{\rho}, \boldsymbol{\phi})\mathbf{s}(f_n) + \mathbf{b}(f_n), \quad (1)$$

where,  $n = 1, \dots, L$ ,  $\mathbf{r}(f_n, \boldsymbol{\theta}, \boldsymbol{\rho}, \boldsymbol{\phi})$  is the Fourier transforms of the array output vector,  $\mathbf{s}(f_n)$  is the vector of object signals,  $\mathbf{b}(f_n)$  is the vector of white Gaussian noise of variance  $\sigma^2(f_n)$ ,  $\mathbf{A}_p(f_n, \boldsymbol{\theta}, \boldsymbol{\rho}, \boldsymbol{\phi})$  is the transfer matrix which is given by

$$\mathbf{A}_p(f_n, \boldsymbol{\theta}, \boldsymbol{\rho}, \boldsymbol{\phi}) = [\mathbf{a}(f_n, \boldsymbol{\theta}_1, \boldsymbol{\rho}_1), \dots, \mathbf{a}(f_n, \boldsymbol{\theta}_P, \boldsymbol{\rho}_P)], \quad (2)$$

$\mathbf{a}(f_n, \boldsymbol{\theta}_k, \boldsymbol{\rho}_k)$  is given by,

$$\mathbf{a}(f_n, \boldsymbol{\theta}_k, \boldsymbol{\rho}_k) = [a(f_n, \boldsymbol{\theta}_{k1}, \boldsymbol{\rho}_{k1}), \dots, e^{-j(\phi_{N-1})} a(f_n, \boldsymbol{\theta}_{kN}, \boldsymbol{\rho}_{kN})]^T, \quad (3)$$

where  $k = 1, \dots, P$ ,  $\phi_i$  represents the phase error associated to the random moving of the  $i^{th}$  sensor from its original position (we assume that the first sensor does not move).  $\boldsymbol{\theta}_k$  and  $\boldsymbol{\rho}_k$  are the bearing and the range of the  $k^{th}$  object to the first sensor of the array, thus,  $\boldsymbol{\theta}_k = \boldsymbol{\theta}_{k1}$  and  $\boldsymbol{\rho}_k = \boldsymbol{\rho}_{k1}$ .  $a(f_n, \boldsymbol{\theta}_{ki}, \boldsymbol{\rho}_{ki})$  is the exact solution of the acoustic scattered field by a spherical shell [3], given by

$$a(f_n, \boldsymbol{\theta}_{ki}, \boldsymbol{\rho}_{ki}) = \frac{P_{s0} \sum_{m=0}^{\infty} j^m (2m+1) B_m h_m^{(1)}(k_n \boldsymbol{\rho}_{ki})}{P_m(\cos(\pi - \boldsymbol{\theta}_{ki} - \boldsymbol{\theta}_{inc}))}, \quad (4)$$

where  $p_{s0}$  is a constant,  $B_m$  is a coefficient depending on limits conditions and  $m$  is the number of modes,  $h_m^{(1)}$  represents the spherical Hankel function.  $K_n = \frac{2\pi f_n}{c}$  where  $K_n$  is the wavenumber and  $c$  is the sound velocity.

The spectral matrix  $\Gamma(f_n, \theta, \rho, \phi)$  is formed for each narrow-band data in each frequency bin and given by

$$\Gamma(f_n, \theta, \rho, \phi) = \begin{matrix} \mathbf{A}_p(f_n, \theta, \rho, \phi) \Gamma_s(f_n) \\ \mathbf{A}_p^+(f_n, \theta, \rho, \phi) + \sigma^2(f_n) \mathbf{I}, \end{matrix} \quad (5)$$

where,  $\Gamma_s(f_n)$  is the spectral matrix associated to the object signals and  $\mathbf{I}$  is the identity matrix.

The frequency diversity is employed, in order to decorre-

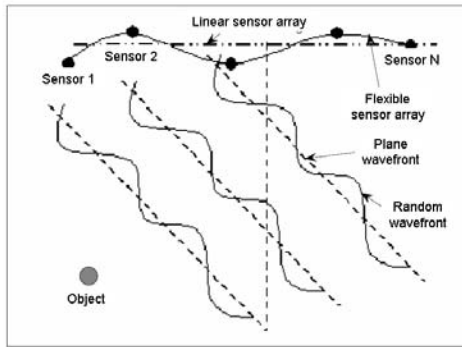


Figure 1: Problem configuration.

late the signals [9]. The idea is to use the bilinear focusing operator [11], to transform the narrowband data in each frequency bin into a single reference frequency bin  $f_0$ . Then, the average of the focused matrices is given by

$$\bar{\Gamma}(f_0, \theta, \rho, \phi) = \frac{1}{L} \sum_{n=1}^L \mathbf{T}(f_0, f_n) \Gamma(f_n, \theta, \rho, \phi) \mathbf{T}^+(f_0, f_n), \quad (6)$$

where  $\mathbf{T}(f_0, f_n)$  is the bilinear focusing operator [11] and  $f_0$  is the focusing frequency chosen in the frequency band on interest. Finally, the spatial spectrum is given by

$$Z(\theta_k, \rho_k) = |\mathbf{a}(f_0, \theta_k, \rho_k) \mathbf{C}(\phi) \bar{\mathbf{V}}_b(f_0)|^{-2}, \quad (7)$$

where  $\mathbf{C}$  is a diagonal matrix containing the sensor phase errors, given by,

$$\mathbf{C}(\phi) = \text{diag}[1, e^{-j(\phi_1)}, \dots, e^{-j(\phi_{N-1})}],$$

$\bar{\mathbf{V}}_b(f_0)$  is the eigenvector matrix of  $\bar{\Gamma}(f_0, \theta, \rho, \phi)$  associated to the smallest eigenvalues. The goal of our method is to estimate simultaneously these phase errors and the object bearings and ranges. Thus, we use the orthogonality property between the source subspace and the noise subspace to form an objective function to minimize using the DIRECT algorithm.

### 3. OBJECTIVE FUNCTION

The DIRECT optimization algorithm was first introduced in [4], motivated by a modification to Lipschitzian optimization. It was created in order to solve difficult global optimization problems with bound constraints and a real-valued

objective function.

DIRECT is an iterative algorithm. That is, it requires no knowledge of the objective function gradient. Instead, the algorithm samples points in the domain, and uses the information it has obtained to decide where to search next. The DIRECT method has been shown to be very competitive with existing algorithms in its class [4]. The strengths of DIRECT lie in the balanced effort it gives to local and global searches, and the few parameters it requires to run. The objective function, that we minimize using the DIRECT optimization algorithm [4], is based on the orthogonality between the two subspaces defined above and it is given by

$$F(\theta, \rho, \phi_1, \dots, \phi_{N-1}) = |\mathbf{a}^+(f_0, \theta, \rho) \mathbf{C}(\phi_1, \dots, \phi_{N-1}) \bar{\mathbf{V}}_b|^2, \quad (8)$$

Note that Eq. (8) is Lipschitzian [4] and satisfies the following condition [4]

$$|F(\Phi) - F(\Phi')| \leq \beta |\Phi - \Phi'|, \quad (9)$$

where  $\Phi = [\theta, \rho, \phi_1, \dots, \phi_{N-1}]^T$  and  $\Phi' = [\theta', \rho', \phi'_1, \dots, \phi'_{N-1}]^T$  and  $0 < \beta < 1$ .

The proposed method allows us to estimate both the source bearings and the phase errors by minimizing the objective function defined above.

The following is the step-by-step description of the developed method:

- dividing the bearing axis into  $L_\theta$  overlapping intervals of length  $\Delta\theta$ , where each interval  $i$  is defined by:  $[\theta_i - \Delta\theta/2, \theta_i + \Delta\theta/2]$ ,
- dividing the range axis into  $L_\rho$  overlapping intervals of length  $\Delta\rho$ , where each interval  $j$  is defined by:  $[\rho_j - \Delta\rho/2, \rho_j + \Delta\rho/2]$ ,
- form the objective function for each sector  $[\theta_i - \Delta\theta/2, \theta_i + \Delta\theta/2] \times [\rho_j - \Delta\rho/2, \rho_j + \Delta\rho/2]$ , as shown in figure 2, where  $i = 1, \dots, L_\theta$  and  $j = 1, \dots, L_\rho$ :

$$F_{ij}(\theta_i, \rho_j, \phi_{1ij}, \dots, \phi_{N-1ij}) = |\bar{\mathbf{V}}_b^+ \mathbf{a}(\theta_i, \rho_j) \mathbf{C}_{ij}(\phi_{1ij}, \dots, \phi_{N-1ij})|^2,$$

- find  $\theta_i, \rho_j, \phi_{1ij}, \dots, \phi_{N-1ij}$  that minimize the objective function in each sector, using the DIRECT algorithm [4].

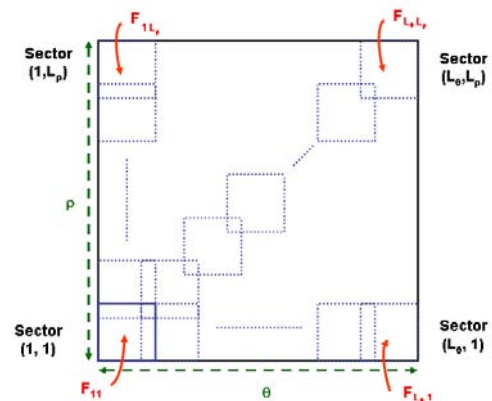


Figure 2: Dividing the space  $\theta, \rho$  into several overlapping sectors.

We notice, after several numerical simulation, that the minimum of the objective function in one sector containing ob-

jects coordinates is smaller than the minimum of that function in an other sector which not containing objects. Thus the idea is to calculate it for all the sectors and to make a thresholding to keep only the smallest objective functions. This assumption will allows us to select only the interesting sectors (those contain object coordinates).

#### 4. EXPERIMENTAL SETUP

Underwater acoustic data have been recorded in an experimental water tank (figure 3) in order to evaluate the performances of the developed method. This tank is filled with water and homogeneous fine sand, where two spherical shells, as shown in figure 4, are buried, between 0 and 0.005 m under the sand. The considered objects have the following characteristics:

- one couple  $(O_1, O_2)$ : spherical shells,  $\theta_a = 0.3$  m,  $\delta = 0.33$  m, full of air,

where  $\delta$  represents the distance between the two objects of the same couple and  $\theta_a$  the outer radius (the inner radius  $\theta_b = \theta_a - 0.001$  m).

The considered objects are made of dural aluminum with density  $D_2 = 1800$  kg/m<sup>3</sup>, the longitudinal and transverse-elastic wave velocities inside the shell medium are  $c_l = 6300$  m/s and  $c_t = 3200$  m/s, respectively. The external fluid is water with density  $D_1 = 1000$  kg/m<sup>3</sup> and the internal fluid is water or air with density  $D_3 = 1.2 \cdot 10^{-6}$  kg/m<sup>3</sup>. We carried out two experiments where the horizontal axis of the transmitter is fixed at 0.45 m from the bottom of the tank with an incident angle  $\theta_{inc} = 60^\circ$  as shown in figure 5 and the receiver moves horizontally, step by step, with a step size  $d = 0.002$  m and takes 10 positions in order to form an array of sensors with  $N = 10$ . The first time, we fixed the receiver horizontal axis at 0.2 m from the bottom of the tank (figure 5), then, we performed one experiment that we named Exp. 1. Then, the horizontal axis of the receiver was fixed at 0.4 m and in the same manner we performed an other experiment that we named Exp. 2. The both experiments are associated to the same couple  $(O_1, O_2)$  of spherical shells. For each experiment, the transmitted signal had the following properties; pulse duration is 15  $\mu$ s, the frequency band is  $[f_{min} = 150, f_{max} = 250]$  kHz, the mid-band frequency is  $f_0 = 200$  kHz and the sampling rate is 2 MHz. The duration of the received signal was 700  $\mu$ s.

At each sensor, time-domain data corresponding only to target echoes are collected with signal to noise ratio equal to 20 dB. The typical sensor output signals recorded during one experiment are shown in figure 6-(a).

#### 5. RESULTS AND DISCUSSION

The first step is to add random phase errors on each sensor output signal. Thus, for the first experiment (Exp. 1) we have used:

$$\phi_a = [0, 0.2, 0.25, 0.37, 0.22, 0.1, 0.05, 0.14, 0.28, 0.35] \text{ radian}$$

For the second experiment (Exp. 2) we have used:

$$\phi_b = [0, 0.6, 0.2, 0.1, 0.52, 1.22, 2.1, 2.9, 3.12, 3.1] \text{ radian.}$$

The experimental data affected by  $\phi_a$  is shown in figure 6-(b). Furthermore, the average of the focused matrices is calcu-

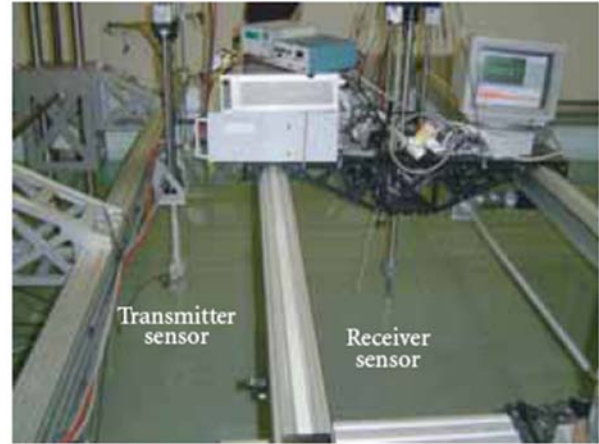


Figure 3: Experimental tank.



Figure 4: Sphere objects.

lated using  $L = 50$  frequencies chosen in the frequency band of interest  $[150, 250]$  kHz and the middle frequency is chosen as the focusing frequency  $f_0 = 200$  kHz.

After several test we have chosen  $\Delta\theta = 12^\circ$  and  $\Delta\rho = 0.05$  m. Then we have calculate the reverse of the objective function for each sector. The obtained values are shown in figure 7. These values form two groups; the first one is associated to the sectors which not contain any object coordinates contrary to the second one.

The obtained bearings and ranges before the correction of the random phase errors are shown in figures 8 and 10. Then, after correction of sensor random phase errors using the minimization of the objective function, the obtained bearings and ranges are shown in figures 9 and 11.

In order to quantize the obtained results, we have calculates the *RootMeanSquareError* (RMSE):  $RMSE_\theta$ ,  $RMSE_\rho$ ,  $RMSE_{\phi_a^{est} - \phi_a^{exp}}$  and  $RMSE_{\phi_b^{est} - \phi_b^{exp}}$ , between the expected  $([\cdot]_{exp})$  and the estimated  $([\cdot]_{est})$  values using the following equations:

$$RMSE_X = \sqrt{\frac{\sum_{i=1}^2 [(X_{exp1} - X_{est1})_i^2 + (X_{exp2} - X_{est2})_i^2]}{4}}, \quad (10)$$

where  $X$  represents  $\theta$  or  $\rho$ ,  $i$  is the experiment and the indexes 1 and 2 represent the first and the second objects of the

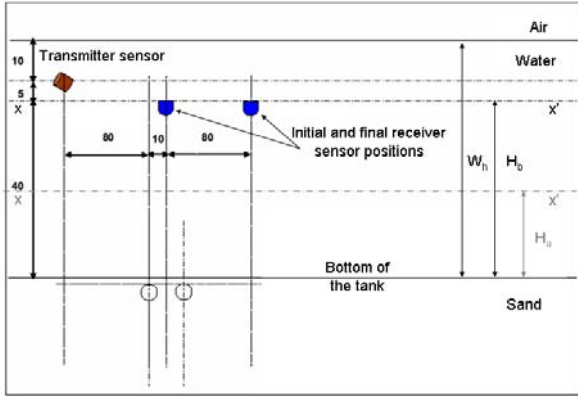


Figure 5: Experimental setup.

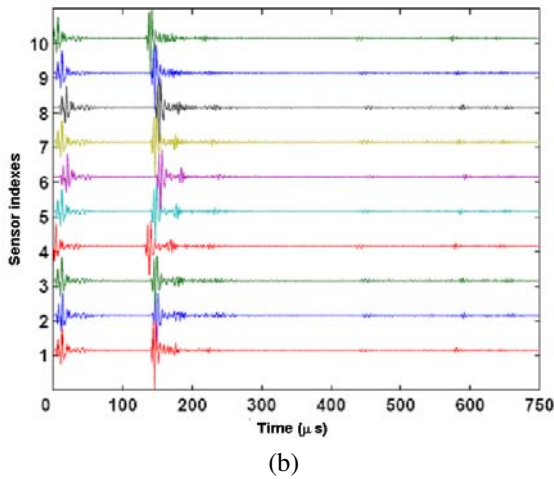
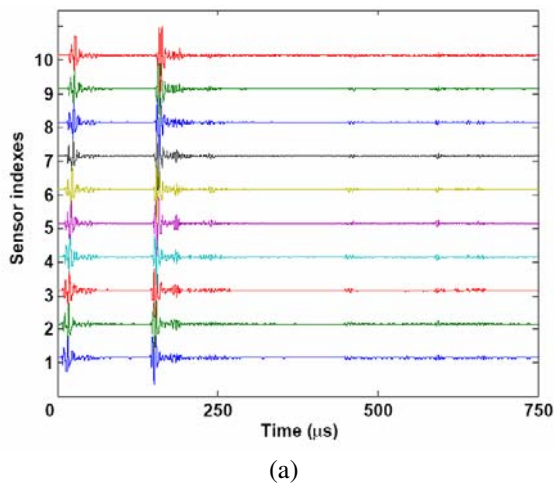


Figure 6: (a) Observed sensor output signals. (b) affected by sensor phase errors  $\phi_a$  and associated to experiment Exp. 1.

couple, respectively.

$$RMSE_{\phi_y^{est}-\phi_y^{exp}} = \sqrt{\frac{\sum_{i=1}^{N-1} [(\phi_i^{est} - \phi_i^{exp})^2]}{N-1}}, \quad (11)$$

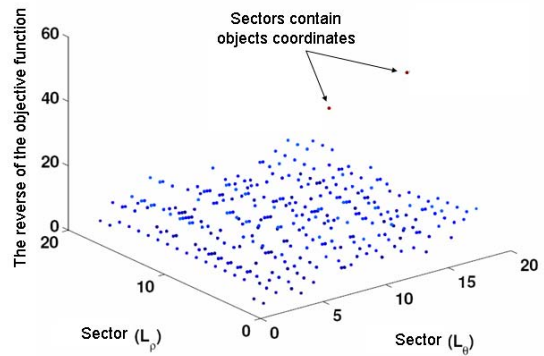


Figure 7: The reverse of the objective function values according to sectors.

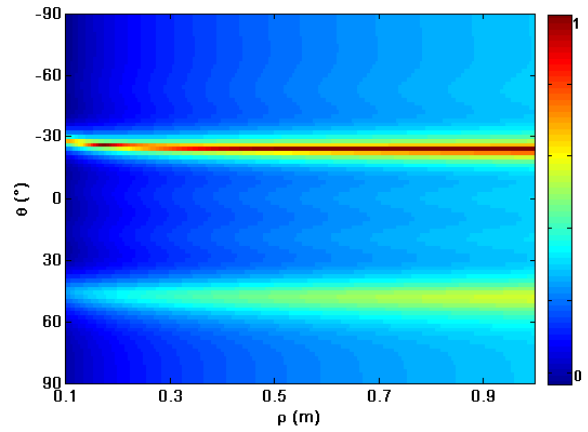


Figure 8: Spatial spectrum in presence of sensor phase errors  $\phi_a$  applied to  $Exp_1$ , before phase errors correction.

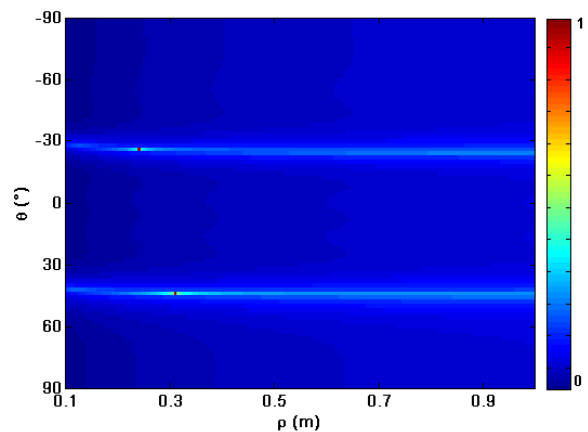


Figure 9: Spatial spectrum in presence of sensor phase errors  $\phi_a$  applied to  $Exp_1$ , after phase errors correction.

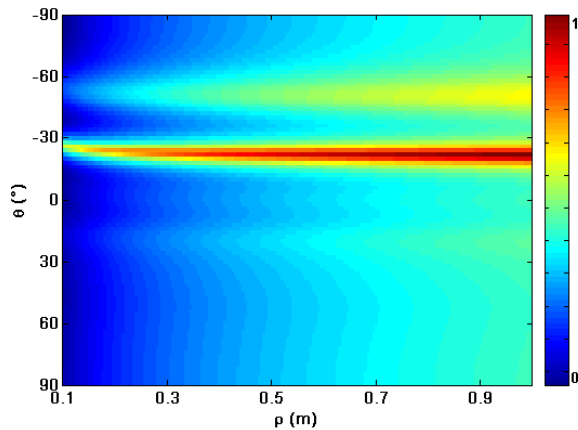


Figure 10: Spatial spectrum in presence of sensor phase errors  $\phi_b$  applied to  $Exp_6$  before phase errors correction.

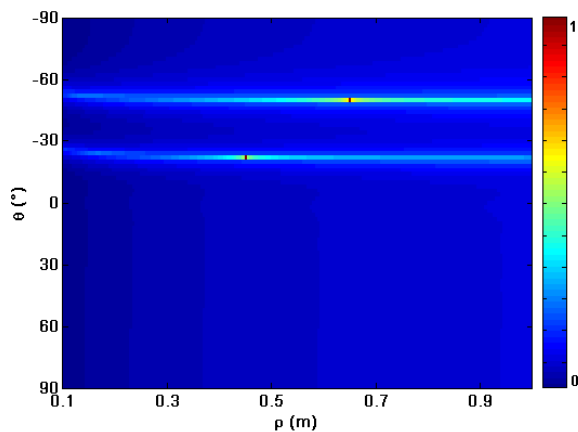


Figure 11: Spatial spectrum in presence of sensor phase errors  $\phi_b$  applied to Exp. 2 after phase errors correction.

where  $y$  represents  $a$  or  $b$  and  $i = 1, \dots, N - 1$ .

The  $RMSE$  obtained values of  $\theta$ ,  $\rho$ ,  $\phi_a$  and  $\phi_b$ , resumed in table 1, show that the  $RMSE$  between the expected and the estimated values remains weak even for high phase errors.

## 6. CONCLUSION

In this study, we have proposed a novel method to estimate both the range and the bearing of buried objects with phase uncertainties. This approach, does not require any prior knowledge of the sensor array shape to be able to correct the data. For that, one combined subspace method with the DIRECT algorithm to estimate simultaneously the object coordinates (bearing and range objects) and the phase errors. The performances of this method are investigated through experimental data affected by random phase errors and associated to many spherical shells buried under the sand. The obtained results are interesting and the  $RMSE$  calculated between the expected and the estimated bearing, range and phase errors remains weak even for high phase errors which shows the effectiveness of the developed method.

## ACKNOWLEDGMENTS

	Exp. 1	Exp. 2
$RMSE_{\theta}$	1.42°	1.45°
$RMSE_{\rho}$	0.03 m	0.04 m
$RMSE_{\phi_a^{est} - \phi_a^{exp}}$ (radian)	0.012	0.01
$RMSE_{\phi_b^{est} - \phi_b^{exp}}$ (radian)	0.013	0.015

Table 1: The  $RMSE$  calculated between the estimated values and the expected values of  $\theta$ ,  $\rho$ ,  $\phi_a$  and  $\phi_b$ .

The authors would like to thank the Dr J. P. Sessarego, from the LMA (Laboratory of Mechanic and Acoustic), Marseille, France, for helpful discussions and technical assistance.

## REFERENCES

- [1] S. Bourennane and M. Frikel, "Localization of wideband sources with estimation of an antenna shape," Proc. IEEE Workshop on Statistical Sig. Array Proc., pp. 97-100, 1996.
- [2] W. Brandenburg, "A point mechanical model for the dynamics of towed arrays", Proc. ICASSP, pp. 40.2.1-40.2.4, 1984.
- [3] R. Goodman and R. Stern, "Reflection and transmission of sound by elastic spherical shells," The Journal of the Acoustical Society of America, vol. 34, no. 3, pp. 338-344, 1962.
- [4] D.R. Jones, C.D. Pertunen and B.E. Stuckman, "Lipschitzian optimisation without the Lipschitz constant," Journal of Optimization and Applications, vol. 79, no. 157-181, 1993.
- [5] S. Marcos, "Calibration of a distorted towed array using a propagation operator," J. Acoust. Soc. Am., vol. 93, no. 4, pp. 1987-1994, 2003.
- [6] Z. Saidi, and S. Bourennane, "Cumulant-based coherent signal subspace method for bearing and range estimation", EURASIP Journal on Advances in Signal Processing, vol. 2007, Article ID 84576, 9 pages, 2007.
- [7] Z. Saidi and S. Bourennane, "Localization of Buried Spherical Shells Based on Wideband Signals", The 31st IEEE International Conference on Acoustics, Speech, and Signal Processing (ICASSP06), pp. 917920, May, Toulouse, France.
- [8] Z. Saidi, S. Bourennane, L. Guillon and P. Sanchez, "Bearing and range estimation using wideband MUSIC method", 13th European Signal Processing Conference, (EUSIPCO'05), Antalya, Turkey, 2005.
- [9] Z. Saidi and S. Bourennane, "Buried objects localization in presence of correlated signals", IEEE Workshop Statistical Signal Processing, Bordeaux, France, 2005.
- [10] R. O. Schmidt, "Multiple emitter location and signal parameter estimation," IEEE Trans. Antennas Propagat., vol. 34, no. 3, pp. 276-280, march 1986.
- [11] S. Valaee and P. Kabal, "Wideband array processing using a two-sided correlation transformation", IEEE Transaction On signal Processing, 43(1), 1995.